

# Reduced Vessel Elasticity Alters Cardiovascular Structure and Function in Newborn Mice

Jessica E. Wagenseil, Chris H. Ciliberto, Russell H. Knutsen, Marilyn A. Levy, Attila Kovacs, Robert P. Mecham

**Abstract**—Elastic blood vessels provide capacitance and pulse-wave dampening, which are critically important in a pulsatile circulatory system. By studying newborn mice with reduced ( $Eln^{+/-}$ ) or no ( $Eln^{-/-}$ ) elastin, we determined the effects of altered vessel elasticity on cardiovascular development and function.  $Eln^{-/-}$  mice die within 72 hours of birth but are viable throughout fetal development when dramatic cardiovascular structural and hemodynamic changes occur. Thus, newborn  $Eln^{-/-}$  mice provide unique insight into how a closed circulatory system develops when the arteries cannot provide the elastic recoil required for normal heart function. Compared with wild type, the  $Eln^{-/-}$  aorta has a smaller unloaded diameter and thicker wall because of smooth muscle cell overproliferation and has greatly reduced compliance. Arteries in  $Eln^{-/-}$  mice are also tortuous with stenoses and dilations. Left ventricular pressure is 2-fold higher than wild type, and heart function is impaired. Newborn  $Eln^{+/-}$  mice, in contrast, have normal heart function despite left ventricular pressures 25% higher than wild type. The major vessels have smaller unloaded diameters and longer lengths. The  $Eln^{+/-}$  aorta has additional smooth muscle cell layers that appear in the adventitia at or just before birth. These results show that the major adaptive changes in cardiovascular hemodynamics and in vessel wall structure seen in the adult  $Eln^{+/-}$  mouse are defined in late fetal development. Together, these results show that reduced elastin in mice leads to adaptive remodeling, whereas the complete lack of elastin leads to pathological remodeling and death. (*Circ Res.* 2009;104:1217-1224.)

**Key Words:** blood pressure ■ cardiovascular physiology ■ development ■ extracellular matrix ■ large artery stiffness

Elastin is a phylogenetically recent protein that imparts elasticity to major vessels in the vertebrate circulatory system. In the low pressure, constant flow circulatory system of invertebrates, elastin is not present and the vessels serve mainly to direct blood flow. In the high pressure, pulsatile flow system of vertebrates, elastin is present and the vessels serve as an elastic reservoir that decreases the systolic load on the heart and provides a constant flow of blood to distal vessels.

The wall in vertebrate elastic vessels is composed of circumferential lamellar units consisting of fenestrated sheets of elastin (elastic laminae), with associated collagen fibers and smooth muscle cells (SMCs). In most mammals, the number of lamellar units is linearly related to wall tension throughout the vascular tree.<sup>1</sup> Lamellar units are organized during fetal development<sup>2</sup> as blood flow and pressure are increasing,<sup>3-6</sup> and the number of units does not change in adult animals. Aortic diameter and wall thickness also increase with blood flow and pressure during development.<sup>7,8</sup> The coordinated changes in wall structure and hemodynamics provide evidence that mechanical signals are critical factors

in determining the structure and organization of vertebrate arteries.

Our previous studies with elastin-insufficient mice show an important relationship between elastin levels, arterial compliance, and cardiovascular function.<sup>9-11</sup> Adult mice with only 1 elastin allele ( $Eln^{+/-}$ ) and hence approximately half the normal elastin levels have higher blood pressure, smaller arteries with thinner walls, altered arterial mechanical behavior, and, surprisingly, an increased number of lamellar units in the vessel wall compared to wild-type (WT) mice. The structural and functional changes in the vessel wall of hypertensive  $Eln^{+/-}$  mice are dramatically different from those that occur in normal vessels exposed to high blood pressure, but this is not attributable to a defect in the hypertensive remodeling response.<sup>12</sup>

We have proposed that the changes in vessel wall structure and cardiovascular hemodynamics in adult  $Eln^{+/-}$  mice are a developmental adaptation to changes in wall stress resulting from altered vascular mechanics caused by reduced elastin amounts. It is not known, however, how early in development these changes occur. To address this question, we assessed

Original received December 3, 2008; revision received April 7, 2009; accepted April 8, 2009.

From the Departments of Cell Biology and Physiology (J.E.W., C.H.C., R.H.K., M.A.L., R.P.M.) and Internal Medicine, Cardiovascular Division (A.K.), Washington University School of Medicine, St Louis, Mo.

Correspondence to Jessica E. Wagenseil, Department of Biomedical Engineering, Saint Louis University, 3507 Lindell Blvd, St Louis, MO 63103. E-mail jwagense@slu.edu

© 2009 American Heart Association, Inc.

*Circulation Research* is available at <http://circres.ahajournals.org>

DOI: 10.1161/CIRCRESAHA.108.192054

blood pressure, blood flow, heart function, vascular structure, and vascular mechanics in newborn mice having 2 (WT, 100% elastin), 1 (*Eln*<sup>+/-</sup>, ≈60% elastin), or 0 (*Eln*<sup>-/-</sup>, 0% elastin) functional elastin alleles. Our findings show that the major structural and hemodynamic changes associated with elastin haploinsufficiency (*Eln*<sup>+/-</sup>) occur during the last few days of gestation and persist into the adult period. We also present the first report of how a closed circulatory system functions when vessels cannot provide the elastic recoil necessary for normal heart operation.

## Materials and Methods

An expanded Materials and Methods section is available in the online data supplement at <http://circres.ahajournals.org>.

Newborn pups between 3 and 24 hours old (postnatal day [P]1) from mice bearing a heterozygous deletion in the elastin gene (*Eln*<sup>+/-</sup>)<sup>10</sup> were used for all studies. All housing, surgical procedures, and experimental protocols were approved by the Institutional Animal Care and Use Committee. Blood pressure was measured with a 30G needle connected to a flow-through pressure transducer and inserted into the left ventricle (LV) using ultrasound visualization. The same ultrasound system was used for echocardiography.<sup>13</sup> After euthanasia, the body and heart weights were measured, the major arteries were imaged, and the ascending aorta was removed. The aorta was processed for electron microscopy or DNA quantification or mounted in a pressure myograph for mechanical studies.<sup>11</sup> After mechanical testing, the unloaded dimensions and residual strain, characterized by the opening angle (OA), were measured from aortic rings. *P*<0.05 was considered significant for all statistical analyses.

## Results

### Reduced Elastin Increases LV Pressure and the Absence of Elastin Impairs Cardiovascular Function

Elastic vessels are critical for proper cardiovascular function in a closed, pulsatile circulatory system. To evaluate the effects of reduced vascular elasticity, we measured LV blood pressure and cardiovascular function in P1 mice with 100%, ≈60%, and 0% elastin levels. We used ultrasound visualization to guide a small gauge needle into the ≈1-mm-diameter LV cavity and recorded blood pressure and heart rate with a fluid-filled catheter system (Figure 1). The increased LV pressure in *Eln*<sup>+/-</sup> and *Eln*<sup>-/-</sup> mice is clear, despite the damped the pressure waveform. The calculated systolic pressure is increased 25% in *Eln*<sup>+/-</sup> and 100% in *Eln*<sup>-/-</sup> mice compared to WT and the heart rates are similar in all genotypes. WT pressures are comparable to previous studies in newborn mice.<sup>3,6,14</sup>

Cardiovascular function was determined by echocardiography and the measured parameters are shown in Table 1. WT and *Eln*<sup>+/-</sup> values are similar to previous studies of newborn mice.<sup>15</sup> *Eln*<sup>-/-</sup> mice show a trend toward increased LV diameter at diastole (a sign of LV dilatation) and increased LV mass. At systole, the inner diameters of the ascending aorta are almost equal in all 3 genotypes (Figure 2). However, the percentage diameter change between systole and diastole is ≈80% less in *Eln*<sup>-/-</sup> ascending aorta than WT and *Eln*<sup>+/-</sup>, indicating a very stiff, noncompliant artery at physiological pressures. Ejection fraction and cardiac output are ≈35% lower in *Eln*<sup>-/-</sup> than WT and *Eln*<sup>+/-</sup>. *Eln*<sup>-/-</sup> mice also show a trend toward decreased blood flow in the proximal ascend-

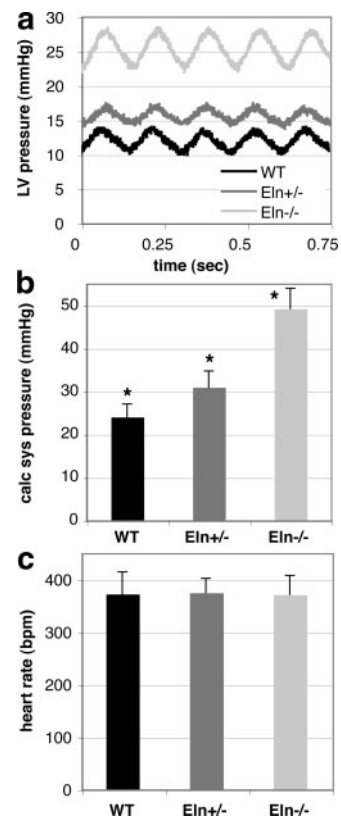


**Figure 1.** Reduced elastin levels correlate with increased LV pressure. Representative LV pressure waveforms (a), average calculated systolic pressure (b), and average heart rates (c) for all genotypes are shown. N=5 (WT and *Eln*<sup>+/-</sup>) and N=3 (*Eln*<sup>-/-</sup>). \**P*<0.05 between all genotypes.

ing aorta, which is consistent with reduced ejection fraction and cardiac output. The maximum physiological shear stress can be calculated from the cardiac output, the aortic inner diameter at systole and by assuming a constant blood viscos-

**Table 1. *Eln*<sup>-/-</sup> Mice Have Impaired Heart Function and Stiff Aortae**

Parameters	WT	<i>Eln</i> <sup>+/-</sup>	<i>Eln</i> <sup>-/-</sup>
<b>M-mode</b>			
LVIDd, mm	1.00±0.18	1.00±0.12	1.29±0.23
LVM, mg	8.7±2.3	8.7±1.7	11.6±3.0
AoIDs, mm	0.53±0.05	0.52±0.08	0.56±0.11
AoDC, %	15.5±3.3	13.6±4.9	3.3±1.7*
<b>Two-dimensional</b>			
EF, %	67±8	65±6	45±16*
CO, mL/min	0.8±0.1	0.8±0.1	0.5±0.2*
<b>Doppler</b>			
AVTI, mm	15.7±3.3	17.1±3.1	11.5±6.4
HR, bpm	433±44	432±32	388±19
N	9	9	5

Data from the echocardiographic studies are shown. LVIDd indicates LV inner diameter at end diastole; LVM, LV mass; AoIDs, ascending aorta inner diameter at end systole; AoDC, ascending aorta percent diameter change between systole and diastole; EF, ejection fraction; CO, cardiac output; AVTI, ascending aorta velocity time integral; HR, heart rate. \**P*<0.05 for *Eln*<sup>-/-</sup> compared to WT and *Eln*<sup>+/-</sup>.

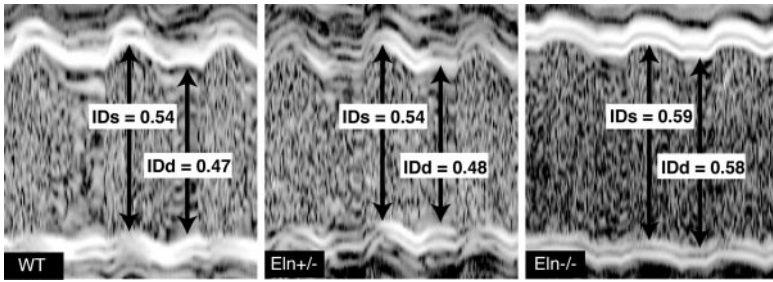


**Figure 2.** The reduced compliance of *Eln*<sup>-/-</sup> ascending aorta is illustrated by representative M-mode images from the echocardiographic studies. Note the small change in inner diameter of the *Eln*<sup>-/-</sup> aorta between end-systole (IDs) (mm) and end-diastole (IDd) (mm) and that all genotypes have approximately the same end-systolic diameter.

ity of 4 cp.<sup>3</sup> The calculated shear stresses are 36, 39 and 19 dyn/cm<sup>2</sup> in WT, *Eln*<sup>+/-</sup>, and *Eln*<sup>-/-</sup> aortae, respectively.

In the echocardiographic studies, the heart rates of anesthetized mice (388±23 bpm) are significantly lower than unanesthetized mice (441±32 bpm), but the heart rates are not significantly different between genotypes. *Eln*<sup>-/-</sup> mice are easily identifiable by their impaired heart function and tortuous, stiff vessels. Movies of the aorta for each genotype are included in the supplemental data (Movie in the online data supplement). Regions of dilation and stenoses are observed for *Eln*<sup>-/-</sup> mice in the ascending and descending aorta and pulmonary artery, as evidenced by abrupt changes in the Doppler flow profiles (Figure 3).

The normalized total heart weight in *Eln*<sup>-/-</sup> mice (8.0±1.5 mg/g) is significantly higher than WT (6.9±0.8 mg/g) and *Eln*<sup>+/-</sup> (7.0±1.0 mg/g). LV hypertrophy, as indicated by the trend toward increased LV mass, is likely responsible for the increase in total heart weight. The body weight is not significantly different between genotypes and averages 1.35±0.18 g for all mice.

**Low Elastin Levels Correlate With Longer Vessels and Altered Cardiovascular Morphology**

Gross morphological analysis of the vascular network in P1 *Eln*<sup>-/-</sup> mice shows longer, tortuous arteries with numerous stenoses and dilations (Figure 3). Variations in the blood flow profile and abrupt changes in arterial diameter are also seen by ultrasound, confirming the presence of stenotic lesions in live animals. In contrast, the basic pattern of *Eln*<sup>+/-</sup> arteries resembles WT with some interesting differences. *Eln*<sup>+/-</sup> arteries have smaller unloaded diameters, longer lengths between branches, and a sharp bend at the right subclavian artery (Figure 3). The average in vivo lengths of WT, *Eln*<sup>+/-</sup>, and *Eln*<sup>-/-</sup> ascending aortae are 1.47±0.08, 1.59±0.08, and

2.38±0.05 mm, respectively, and are significantly different between all genotypes.

**Elastin Deficiency Alters the Arrangement of SMCs in the Vessel Wall**

The gross morphology shows that elastin deficiency changes the geometry and patterning of developing blood vessels. We used electron microscopy to determine the effects of elastin deficiency on the ultrastructural arrangement of SMCs and extracellular matrix (ECM) in the newborn vessel wall (Figure 4). WT aorta looks similar to previous electron microscopic images of newborn rat and mouse aortae<sup>16,17</sup> and has circumferentially arranged SMCs and elastic laminae that extend from the intima through ≈2/3 of the wall thickness. The laminae are not yet continuous but will progressively thicken and become continuous by P7.<sup>2</sup> The thickest laminae are the central units, whereas the layers closest to the intima and adventitia are thinner. The adventitia consists of circumferentially oriented cells within an ECM rich in collagen and proteoglycans. The *Eln*<sup>+/-</sup> aorta has thinner but a higher number of elastic laminae (≈11 compared to ≈8 in WT) that occupy a greater percentage of the vessel wall and extend into the adventitia. The *Eln*<sup>-/-</sup> aorta has SMCs that are highly disorganized compared to WT or *Eln*<sup>+/-</sup>. Cells near the adventitial interface are organized circumferentially, but those in the middle of the wall show various orientations, are surrounded by a collagen-rich matrix, and have few cell-cell interactions. SMCs near the intima have less collagen in the ECM and are oriented longitudinally which, together with increased proliferation and enhanced migration, contributes to obliteration of the arterial lumen.<sup>18</sup> The *Eln*<sup>-/-</sup> aorta has significantly higher DNA amounts (58.5±4.5 ng) than *Eln*<sup>+/+</sup> (48.2±2.4 ng) and *Eln*<sup>+/-</sup> (48.6±3.2 ng) because of the hyperproliferation of SMCs.

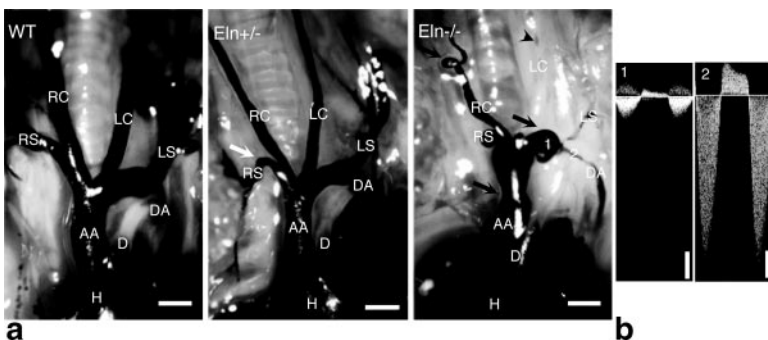


**Figure 3.** Elastin insufficiency alters vascular morphology. The heart (H), ductus arteriosus (D), ascending aorta (AA), right subclavian (RS), right carotid (RC), left carotid (LC), left subclavian (LS), and descending aorta (DA) are labeled in representative morphologic images (a). *Eln*<sup>+/-</sup> arteries have smaller diameters, longer lengths, and a sharp bend at the RS (white arrow). *Eln*<sup>-/-</sup> arteries have stenoses, dilations, and tortuosity (black arrows). The eosin dye did not flow into the *Eln*<sup>-/-</sup> left carotid (LC), but the artery can be identified by blood clots in the stenosed regions (black arrowhead). Scale bars=0.5 mm. Areas 1 and 2 in the *Eln*<sup>-/-</sup> image correspond to regions where the blood flow velocities were measured with Doppler

ultrasound and are shown in b. Low flow (1) is present in the dilated region, and high flow (2) is present in the stenosed region (b). Scale bars=20 cm/sec.

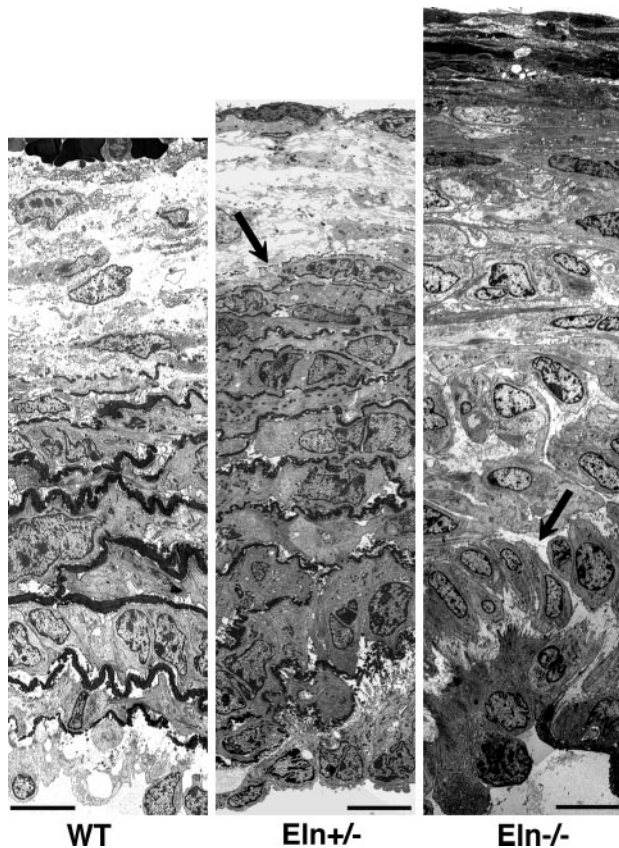


**Figure 4.** *Eln*<sup>+/-</sup> and *Eln*<sup>-/-</sup> mice have unique vascular wall organization. Representative electron microscopic images taken at ×700 original magnification of the proximal ascending aorta in each genotype are shown. The adventitia is at the top of the images. Note the additional elastic laminae near the adventitial interface in *Eln*<sup>+/-</sup> aorta and disorganized SMCs near the intimal interface in *Eln*<sup>-/-</sup> aorta (black arrows). Scale bars=11 μm.

**Mechanical Differences in Vessels With Differing Elastin Levels**

The mechanical properties of the vessel wall, combined with the applied in vivo pressures and forces, produce stresses and strains on the wall that may affect the developmental SMC phenotype. Growth during development can also produce residual stresses and strains in the vessel wall. To determine the mechanical properties and applied stresses and strains in elastin insufficient vessels, we measured the unloaded aortic geometry and OA and performed ex vivo mechanical tests. The unloaded outer diameters are not significantly different between genotypes (Table 2). The unloaded inner diameter is 20% larger and the unloaded thickness is 20% smaller in WT aorta compared to *Eln*<sup>+/-</sup> and *Eln*<sup>-/-</sup>. The circumferential residual strain, characterized by the OA, is 35% smaller in *Eln*<sup>-/-</sup> aorta compared to WT and *Eln*<sup>+/-</sup>.

At all pressures >5 mm Hg, the outer diameter of *Eln*<sup>-/-</sup> aorta is significantly smaller than WT and *Eln*<sup>+/-</sup> (Figure 5). Yet at the systolic pressure for each genotype (Figure 1), the diameters are approximately the same (0.51 to 0.55 mm), as confirmed by the echocardiographic studies (Table 1 and Figure 2). The small diameter change with pressure for *Eln*<sup>-/-</sup> aorta is consistent with the echocardiography data and accounts for the low compliance values. At all pressures

**Table 2. The *Eln*<sup>-/-</sup> Aorta Has Altered Geometry and Decreased Residual Strain**

	WT	<i>Eln</i> <sup>+/-</sup>	<i>Eln</i> <sup>-/-</sup>
OD, mm	0.394±0.021	0.372±0.018	0.375±0.027
ID, mm	0.262±0.026†	0.218±0.018	0.206±0.022
T, mm	0.066±0.004†	0.077±0.006	0.085±0.011
OA, deg	141±12	133±20	88±34*
N	10	12	6

Unloaded dimensions of the ascending aorta. Outer diameter (OD), inner diameter (ID), thickness (T), and OA are shown. \**P*<0.05 for *Eln*<sup>-/-</sup> compared to WT and *Eln*<sup>+/-</sup>; †*P*<0.05 for WT compared to *Eln*<sup>+/-</sup> and *Eln*<sup>-/-</sup>.

<25 mm Hg, *Eln*<sup>-/-</sup> compliance is significantly lower than WT and/or *Eln*<sup>+/-</sup>. The slope of the *Eln*<sup>+/-</sup> pressure–diameter curve is slightly different than WT, which provides altered compliance at some pressures. The axial force data are not shown because at the in vivo length the force remains approximately constant with increasing pressure and the forces are not significantly different between genotypes.

The circumferential stress is significantly lower in *Eln*<sup>-/-</sup> aorta compared to WT and *Eln*<sup>+/-</sup> at all pressures (Figure 6). The axial stress is not significantly different between genotypes at any pressure. At all pressures >5 mm Hg, the circumferential stretch is greater in *Eln*<sup>+/-</sup> aorta than WT and *Eln*<sup>-/-</sup>. At the systolic pressures for each genotype (Figure 1), the circumferential stresses are almost identical in all 3 genotypes, the axial stresses are approximately double in *Eln*<sup>-/-</sup> aorta compared to WT and *Eln*<sup>+/-</sup>, and the circumferential stretch ratio is ≈10% higher in *Eln*<sup>+/-</sup> aorta compared to WT and *Eln*<sup>-/-</sup>.

**Discussion**

Blood flow and pressure increase rapidly during the mid-embryonic and early postnatal stages in mice and most

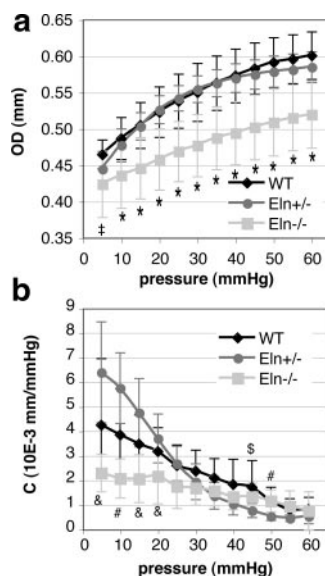


**Figure 5.** *Eln*<sup>-/-</sup> mice have reduced aortic diameter and compliance in vitro. Average outer diameter (OD) (a) and average compliance (C) (b) vs pressure. N=10 (WT), N=12 (*Eln*<sup>+/-</sup>), and N=6 (*Eln*<sup>-/-</sup>). \**P*<0.05 for *Eln*<sup>-/-</sup> compared to WT and *Eln*<sup>+/-</sup>; †*P*<0.05 between WT and *Eln*<sup>-/-</sup>; &*P*<0.05 between *Eln*<sup>+/-</sup> and *Eln*<sup>-/-</sup>; \$*P*<0.05 between WT and *Eln*<sup>+/-</sup>; #*P*<0.05 for *Eln*<sup>+/-</sup> compared to WT and *Eln*<sup>-/-</sup>.

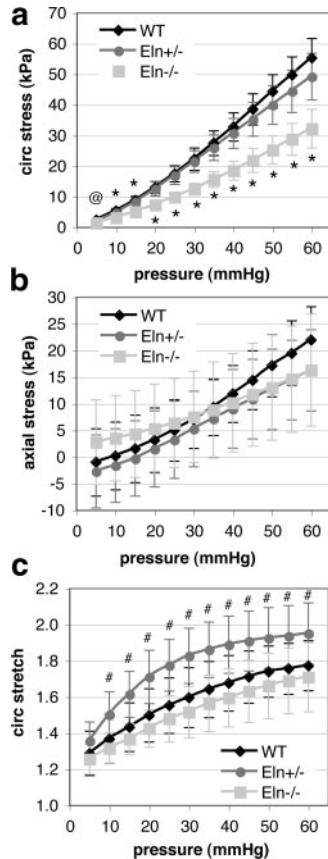


**Figure 6.** *Eln*<sup>-/-</sup> aorta has altered circumferential stresses, and *Eln*<sup>+/-</sup> aorta has altered circumferential stretch ratios. Average circumferential stress (a), axial stress (b), and circumferential stretch ratio (c) vs pressure are shown. N=10 (WT), N=12 (*Eln*<sup>+/-</sup>), and N=6 (*Eln*<sup>-/-</sup>). @*P*<0.05 between all genotypes; \**P*<0.05 for *Eln*<sup>-/-</sup> compared to WT and *Eln*<sup>+/-</sup>; #*P*<0.05 for *Eln*<sup>+/-</sup> compared to WT and *Eln*<sup>-/-</sup>.

vertebrates.<sup>3-6</sup> Concurrent with these hemodynamic changes are alterations in vessel wall maturation exemplified by increased expression of the structural ECM proteins elastin and the fibrillar collagens.<sup>18-20</sup> The correlation between changing hemodynamics and ECM expression suggests that vascular SMCs adjust the amounts and types of ECM molecules they produce in response to wall stress and other mechanical signals. Indeed, increases in blood flow and pressure can only occur to the extent that structural modifications of the vessel wall can accommodate the hemodynamic changes. This suggests an essential feedback mechanism whereby changing vascular structure/function during development regulates cardiac hemodynamics, and vice versa.

### Cardiovascular Properties of Newborn Mice With no Elastin (*Eln*<sup>-/-</sup>)

Because *Eln*<sup>-/-</sup> mice are viable throughout fetal development when many of the critical cardiovascular structural and hemodynamic changes are occurring, they provide unique insight into how a closed circulatory system develops when vertebrate vessels cannot provide the elastic recoil required for normal heart function. Newborn *Eln*<sup>-/-</sup> mice have tortuous, stenotic arteries that show little diameter change between systole and diastole. Without elastic arteries, LV pressure

increases in an attempt to maintain cardiac output and perfusion pressure through the smaller, stiffer *Eln*<sup>-/-</sup> aorta. The high blood pressure and increased afterload lead to cardiac hypertrophy and impaired cardiac function.

Although hypertrophic cardiac remodeling is expected with high blood pressure and noncompliant vessels, it is remarkable that cardiac development proceeds to birth with arteries as stiff and tortuous as those in *Eln*<sup>-/-</sup> mice. Based on morphological comparison, however, most of the adverse changes in vessel wall structure occur during the last few days of development. At embryonic day (E)15.5, the aortae in WT and *Eln*<sup>-/-</sup> mice look similar by histology and both have ≈8 circumferential cell layers.<sup>18</sup> There is little elastin or collagen in the wall at this stage, so the stresses are borne mostly by the cells. Because wall structure is similar, hemodynamic forces are most likely similar in the 2 genotypes. There is a dramatic increase in elastin and collagen production beginning around E15,<sup>21,22</sup> which suggests that the wall is strengthening in response to increased hemodynamic stimuli. When elastin cannot be produced at appropriate levels to accommodate increased wall stress, as in the *Eln*<sup>-/-</sup> aorta, SMCs proliferate to lower the wall stress by increasing the wall thickness. As a result, at P1, the physiological circumferential stress in the thicker *Eln*<sup>-/-</sup> aorta is approximately equal to WT, despite the almost 2-fold higher LV pressure in *Eln*<sup>-/-</sup> mice. *Eln*<sup>-/-</sup> SMCs proliferate at the inner wall of the aorta, increasing the thickness as well decreasing the inner diameter, which partially normalizes the reduced shear stress caused by decreased cardiac output. For reasons that are not yet understood, SMC proliferation continues in the *Eln*<sup>-/-</sup> aorta until the lumen becomes occluded and the animal dies.

The similarity in structure between WT and *Eln*<sup>-/-</sup> aorta at E15.5 shows that elastin is not necessary for the recruitment of SMCs to the developing aortic wall nor is it required for their initial circumferential organization. It may, however, play an important role in maintaining the layered architecture by providing a direct signal to SMCs<sup>23,24</sup> or, in its polymerized form, creating a physical barrier and/or landmark that serves to spatially compartmentalize SMCs. By P1, the elastic laminae are almost continuous in WT aorta and each SMC is in contact with the elastin above and below it in the wall.<sup>17</sup> The loss of this physical restraint in vessels without elastin may contribute to the changes in SMC organization and phenotype observed in *Eln*<sup>-/-</sup> mice. In vitro, mechanical strain induces proliferation in SMCs plated on collagen, fibronectin, and vitronectin, but not on elastin or laminin, suggesting that ECM-specific signals and mechanical strain and/or stress work coordinately to alter SMC phenotype.<sup>25</sup>

### Newborn Mice With Reduced Elastin Levels (*Eln*<sup>+/-</sup>)

In contrast to the altered cardiac function in *Eln*<sup>-/-</sup> mice, functional parameters in newborn *Eln*<sup>+/-</sup> mice are comparable to WT values. The heart shows normal ejection fraction and cardiac output, despite longer arteries with smaller unloaded diameters. As adults, *Eln*<sup>+/-</sup> mice have increased stroke volume and cardiac output,<sup>9</sup> suggesting that the *Eln*<sup>+/-</sup> cardiovascular system continues to remodel after birth. The outer diameters of newborn *Eln*<sup>+/-</sup> and WT aorta are not

significantly different at any pressure, but the outer diameter of adult *Eln*<sup>+/-</sup> aorta is significantly smaller than WT at most pressures,<sup>9,11</sup> again suggesting additional changes after birth. Although newborn *Eln*<sup>+/-</sup> mice have higher LV pressures than WT, the pressure increase is lower than what is seen in *Eln*<sup>-/-</sup> mice. The 25% pressure difference between *Eln*<sup>+/-</sup> and WT mice at P1 is similar to the pressure difference in adult mice<sup>9,11</sup>; therefore this major hemodynamic parameter is established in *Eln*<sup>+/-</sup> mice before birth and persists into adulthood. The pressure increase at birth, combined with both pre- and postnatal remodeling, allows *Eln*<sup>+/-</sup> mice to develop unique cardiovascular structure and hemodynamic parameters that are “normal” for this genotype. At this new cardiovascular set point, adult *Eln*<sup>+/-</sup> mice are able to maintain cardiac and cardiovascular function despite significantly smaller arteries and a lifetime of increased blood pressure. This is accomplished without the pathological vessel wall remodeling observed in adult onset hypertension. The initial conditions that determine this cardiovascular set point also allow for a modified aging process in *Eln*<sup>+/-</sup> arteries,<sup>26</sup> showing that developmental modifications have consequences throughout the lifespan of the animal.

One of the unique features of adult *Eln*<sup>+/-</sup> arteries is an increased number of SMC layers and elastic laminae in the vessel wall.<sup>10</sup> In this study, we show that these layers are present at birth and appear in the adventitia. We have speculated that in elastin insufficiency, SMCs cannot make enough elastin to accommodate circumferential forces, and the increased number of lamellar units is a developmental adaptation to normalize wall tension.<sup>9</sup> The elevated blood pressure in newborn *Eln*<sup>+/-</sup> mice supports our hypothesis; higher pressure means higher wall tension, but the addition of 3 lamellar units to the wall brings tension per lamellar unit back to within 10% of WT values.

The extra SMC layers in the *Eln*<sup>+/-</sup> aorta are associated with a decrease in adventitial area, suggesting that adventitial cells give rise to these structures. Numerous studies show that the adventitia is important in sensing wall stress and that adventitial cells can be activated in response to hypertension or other forms of vascular injury.<sup>27</sup> During development, *Eln*<sup>+/-</sup> vessels experience more circumferential stretch than WT with each cardiac cycle because of their increased pressure and smaller inner diameters. The increased stretch could trigger adventitial cells to differentiate into SMCs that produce extra layers of elastin. Recent findings show that the adventitia contains a progenitor cell population capable of differentiating into SMCs that repopulate the wall.<sup>28,29</sup> These cells appear in the adventitia in late embryonic and early postnatal development,<sup>29</sup> at the same time that large hemodynamic and structural changes are occurring in the vessel wall.

### Axial Stress, Tortuosity, and Residual Strain

Axial stress in arteries is often neglected, but there is increasing evidence that arteries remodel to normalize axial tension and the resulting stresses.<sup>30,31</sup> Arteries can grow in response to increased axial tension but cannot shorten and will actually grow and become tortuous with decreased axial tension.<sup>32</sup> Tension is regulated by the amount of axial stretch

applied to each vessel in vivo. The estimated in vivo stretch ratio of all P1 aortae in this study is 1.01. This is lower than the stretch ratio in adult WT and *Eln*<sup>+/-</sup> aortae,<sup>11</sup> but the stretch ratio is known to increase with postnatal development in mice.<sup>3</sup> Gross morphological analysis found that *Eln*<sup>-/-</sup> arteries have increased length and are tortuous, implying that they grew in response to decreased axial tension at some point during development. Similar, but less extreme, vascular abnormalities occur in *Eln*<sup>+/-</sup> arteries and other mouse models where elastic fiber structure or assembly is perturbed through gene inactivation.<sup>11,33–35</sup> Removing elastin by treatment with elastase eliminates the axial traction force, whereas treatment with collagenase has no effect.<sup>36</sup> Therefore, it is possible that arteries lacking elastin cannot sustain the required axial tension necessary for normal, nontortuous development.

Arteries experience circumferential residual strain that may be caused by differential growth at the inner and outer wall and serves to normalize the transmural strains.<sup>37,38</sup> The OA in adult *Eln*<sup>+/-</sup> aorta is larger than WT, but the intramural strain distributions are almost identical at physiological pressures.<sup>11</sup> The OA in P1 *Eln*<sup>+/-</sup> aorta is not significantly different from WT, but OA may be another parameter that changes in postnatal remodeling. The P1 *Eln*<sup>-/-</sup> aorta, in contrast, has a significantly smaller OA than WT and *Eln*<sup>+/-</sup> aortae. This is contrary to the increased OA in normal adult vessels with increased pressure and with increased SMC growth at the intimal surface.<sup>12,39,40</sup> The unexpected decrease in *Eln*<sup>-/-</sup> OA shows that ECM is an important component in growth models for residual strain and that developmental adaptations should be treated differently than adult remodeling.

The average OA and geometry were used to calculate the transmural strain distribution for each genotype. WT and *Eln*<sup>+/-</sup> aortae have 5 to 9% higher strains at the outer wall compared to the inner wall, whereas *Eln*<sup>-/-</sup> aorta has 6% higher strains at the inner wall compared to the outer wall. The increased strain and consequently increased stress at the inner wall may contribute to the medial hyperplasia in the *Eln*<sup>-/-</sup> aorta.

### Stenotic Lesions and Elastin Levels

The aortic stenoses in *Eln*<sup>-/-</sup> mice arise from medial, not intimal hyperplasia, which is similar to the pathology seen in stenotic lesions in humans with supravalvular aortic stenosis (SVAS) (Online Mendelian Inheritance of Man no. 185500). SVAS is caused by loss of function mutations that lead to functional elastin haploinsufficiency.<sup>41</sup> Humans and mice respond to elastin haploinsufficiency differently: humans develop focal stenotic lesions in the aorta and other great vessels, whereas there is a general narrowing of arterial vessels without focal lesions in mice. Stenoses have been observed, however, in adult hBAC-mNULL mice with elastin levels ≈30% of normal.<sup>42</sup> Adult hBAC-mNULL mice have mean pressures ≈50 mm Hg higher than WT, whereas adult *Eln*<sup>+/-</sup> mice have mean pressures ≈40 mm Hg higher.<sup>11</sup> There may be a threshold combination of decreased elastin and increased blood pressure that determines whether the developmental vessel wall remodeling is advantageous or pathological, and the threshold may be different in humans

and mice. Characterizing this delicate balance between elastin levels, mechanical stimuli, SMC phenotype, and aortic wall structure will be important in developing strategies for treating and preventing stenotic lesions in SVAS.

## Conclusion

Our results show that vascular elasticity is essential for vessel wall development and cardiovascular function in vertebrates. Without elastic vessels to provide an elastic reservoir, high blood pressure and stiff, stenotic arteries cause impaired LV function in newborn *Eln*<sup>-/-</sup> mice. The high blood pressure and stiff vessels also lead to SMC proliferation and vessel lumen narrowing as the cells attempt to normalize wall stress by increasing wall thickness. In the absence of elastin to provide an axial traction force, the arteries become longer and tortuous, which only increases the afterload on the heart. Thus, without elastin, a closed, pulsatile, high pressure circulatory system cannot operate. When elastin content is reduced to ≈60% in mice, however, the developing cardiovascular system can adapt to produce normal cardiac function despite significant changes in the vessel wall structure, mechanics, and hemodynamics. The major adaptations occur in late fetal development and persist into adulthood, defining a new cardiovascular set point for these mice. This functional adaptation can only occur when the ECM is being formed and appropriate gene sets are being expressed.

## Acknowledgments

We thank Dean Li at the University of Utah for providing the *Eln*<sup>+/-</sup> mice and the Mouse Cardiovascular Phenotyping Core at Washington University for assistance with the echocardiographic studies.

## Sources of Funding

This research was funded by NIH grants HL087563 (to J.E.W.); and HL53325, HL74138, and HL084922 (to R.P.M.).

## Disclosures

None.

## References

- Wolinsky H, Glagov S. A lamellar unit of aortic medial structure and function in mammals. *Circ Res*. 1967;20:99–111.
- Davis EC. Elastic lamina growth in the developing mouse aorta. *J Histochem Cytochem*. 1995;43:1115–1123.
- Huang Y, Guo X, Kassab GS. Axial nonuniformity of geometric and mechanical properties of mouse aorta is increased during postnatal growth. *Am J Physiol Heart Circ Physiol*. 2006;290:H657–H664.
- Ishiwata T, Nakazawa M, Pu WT, Tevosian SG, Izumo S. Developmental changes in ventricular diastolic function correlate with changes in ventricular myoarchitecture in normal mouse embryos. *Circ Res*. 2003;93:857–865.
- Keller BB, MacLennan MJ, Tinney JP, Yoshigi M. In vivo assessment of embryonic cardiovascular dimensions and function in day-10.5 to -14.5 mouse embryos. *Circ Res*. 1996;79:247–255.
- Wiesmann F, Ruff J, Hiller KH, Rommel E, Haase A, Neubauer S. Developmental changes of cardiac function and mass assessed with MRI in neonatal, juvenile, and adult mice. *Am J Physiol Heart Circ Physiol*. 2000;278:H652–H657.
- Hudlicka O, Tyler K. Growth of vessels during pre- and postnatal development. In: *Angiogenesis: The Growth of the Vascular System*. London, United Kingdom: Academic Press; 1986:41–66.
- Langille BL. Arterial remodeling: Relation to hemodynamics. *Can J Physiol Pharmacol*. 1996;74:834–841.
- Faury G, Pezet M, Knutsen RH, Boyle WA, Heximer SP, McLean SE, Minkes RK, Blumer KJ, Kovacs A, Kelly DP, Li DY, Starcher B, Mecham RP. Developmental adaptation of the mouse cardiovascular system to elastin haploinsufficiency. *J Clin Invest*. 2003;112:1419–1428.
- Li DY, Faury G, Taylor DG, Davis EC, Boyle WA, Mecham RP, Stenzel P, Boak B, Keating MT. Novel arterial pathology in mice and humans hemizygous for elastin. *J Clin Invest*. 1998;102:1783–1787.
- Wagenseil JE, Nerurkar NL, Knutsen RH, Okamoto RJ, Li DY, Mecham RP. Effects of elastin haploinsufficiency on the mechanical behavior of mouse arteries. *Am J Physiol Heart Circ Physiol*. 2005;289:H1209–H1217.
- Wagenseil JE, Knutsen RH, Li D, Mecham RP. Elastin insufficient mice show normal cardiovascular remodeling in 2K1C hypertension, despite higher baseline pressure and unique cardiovascular architecture. *Am J Physiol Heart Circ Physiol*. 2007;293:H574–H582.
- Lai L, Leone TC, Zechner C, Schaeffer PJ, Kelly SM, Flanagan DP, Medeiros DM, Kovacs A, Kelly DP. Transcriptional coactivators pgc-1alpha and pgc-1beta control overlapping programs required for perinatal maturation of the heart. *Genes Dev*. 2008;22:1948–1961.
- Ishii T, Kuwaki T, Masuda Y, Fukuda Y. Postnatal development of blood pressure and baroreflex in mice. *Auton Neurosci*. 2001;94:34–41.
- Bose AK, Mathewson JW, Anderson BE, Andrews AM, Martin Gerdes A, Benjamin Perryman M, Grossfeld PD. Initial experience with high frequency ultrasound for the newborn c57bl mouse. *Echocardiography*. 2007;24:412–419.
- Cliff WJ. The aortic tunica media in growing rats studied with the electron microscope. *Lab Invest*. 1967;17:599–615.
- Davis EC. Smooth muscle cell to elastic lamina connections in developing mouse aorta. Role in aortic medial organization. *Lab Invest*. 1993;68:89–99.
- Li DY, Brooke B, Davis EC, Mecham RP, Sorensen LK, Boak BB, Eichwald E, Keating MT. Elastin is an essential determinant of arterial morphogenesis. *Nature*. 1998;393:276–280.
- Bendeck MP, Keeley FW, Langille BL. Perinatal accumulation of arterial wall constituents: relation to hemodynamic changes at birth. *Am J Physiol*. 1994;267:H2268–H2279.
- Looker T, Berry CL. The growth and development of the rat aorta. II. Changes in nucleic acid and scleroprotein content. *J Anat*. 1972;113:17–34.
- Kelleher CM, McLean SE, Mecham RP. Vascular extracellular matrix and aortic development. *Curr Top Dev Biol*. 2004;62:153–188.
- McLean SE, Mecham BH, Kelleher CM, Mariani TJ, Mecham RP. Extracellular matrix gene expression in the developing mouse aorta. In: Miner JH, ed. *Extracellular Matrices and Development*. Vol 15. New York: Elsevier; 2005:82–128.
- Karnik SK, Brooke BS, Bayes-Genis A, Sorensen L, Wythe JD, Schwartz RS, Keating MT, Li DY. A critical role for elastin signaling in vascular morphogenesis and disease. *Development*. 2003;130:411–423.
- Mochizuki S, Brassart B, Hinek A. Signaling pathways transduced through the elastin receptor facilitate proliferation of arterial smooth muscle cells. *J Biol Chem*. 2002;277:44854–44863.
- Wilson E, Sudhir K, Ives HE. Mechanical strain of rat vascular smooth muscle cells is sensed by specific extracellular matrix/integrin interactions. *J Clin Invest*. 1995;96:2364–2372.
- Pezet M, Jacob MP, Escoubet B, Gheduzzi D, Tillet E, Perret P, Huber P, Quaglini D, Vranckx R, Li DY, Starcher B, Boyle WA, Mecham RP, Faury G. Elastin haploinsufficiency induces alternative aging processes in the aorta. *Rejuvenation Res*. 2008;11:97–112.
- Stenmark KR, Davie N, Frid M, Gerasimovskaya E, Das M. Role of the adventitia in pulmonary vascular remodeling. *Physiology (Bethesda)*. 2006;21:134–145.
- Hu Y, Zhang Z, Torsney E, Afzal AR, Davison F, Metzler B, Xu Q. Abundant progenitor cells in the adventitia contribute to atherosclerosis of vein grafts in apoE-deficient mice. *J Clin Invest*. 2004;113:1258–1265.
- Passman JN, Dong XR, Wu SP, Maguire CT, Hogan KA, Bautch VL, Majesky MW. A sonic hedgehog signaling domain in the arterial adventitia supports resident sca1+ smooth muscle progenitor cells. *Proc Natl Acad Sci U S A*. 2008;105:9349–9354.
- Dye WW, Gleason RL, Wilson E, Humphrey JD. Altered biomechanical properties of carotid arteries in two mouse models of muscular dystrophy. *J Appl Physiol*. 2007;103:664–672.
- Jackson ZS, Gotlieb AI, Langille BL. Wall tissue remodeling regulates longitudinal tension in arteries. *Circ Res*. 2002;90:918–925.

32. Jackson ZS, Dajnowiec D, Gotlieb AI, Langille BL. Partial off-loading of longitudinal tension induces arterial tortuosity. *Arterioscler Thromb Vasc Biol.* 2005;25:957–962.
33. Hanada K, Vermeij M, Garinis GA, de Waard MC, Kunen MG, Myers L, Maas A, Duncker DJ, Meijers C, Dietz HC, Kanaar R, Essers J. Perturbations of vascular homeostasis and aortic valve abnormalities in fibulin-4 deficient mice. *Circ Res.* 2007;100:738–746.
34. Nakamura T, Lozano PR, Ikeda Y, Iwanaga Y, Hinek A, Minamisawa S, Cheng CF, Kobuke K, Dalton N, Takada Y, Tashiro K, Ross J Jr, Honjo T, Chien KR. Fibulin-5/dance is essential for elastogenesis in vivo. *Nature.* 2002;415:171–175.
35. Yanagisawa H, Davis EC, Starcher BC, Ouchi T, Yanagisawa M, Richardson JA, Olson EN. Fibulin-5 is an elastin-binding protein essential for elastic fibre development in vivo. *Nature.* 2002;415:168–171.
36. Dobrin PB, Schwarcz TH, Mrkvicka R. Longitudinal retractive force in pressurized dog and human arteries. *J Surg Res.* 1990;48:116–120.
37. Fung YC. What are the residual stresses doing in our blood vessels? *Ann Biomed Eng.* 1991;19:237–249.
38. Taber LA, Humphrey JD. Stress-modulated growth, residual stress, and vascular heterogeneity. *J Biomech Eng.* 2001;123:528–535.
39. Fridez P, Makino A, Miyazaki H, Meister JJ, Hayashi K, Stergiopoulos N. Short-term biomechanical adaptation of the rat carotid to acute hypertension: contribution of smooth muscle. *Ann Biomed Eng.* 2001;29:26–34.
40. Matsumoto T, Hayashi K. Stress and strain distribution in hypertensive and normotensive rat aorta considering residual strain. *J Biomech Eng.* 1996;118:62–73.
41. Li DY, Toland AE, Boak BB, Atkinson DL, Ensing GJ, Morris CA, Keating MT. Elastin point mutations cause an obstructive vascular disease, supravalvular aortic stenosis. *Hum Mol Genet.* 1997;6:1021–1028.
42. Hirano E, Knutsen RH, Sugitani H, Ciliberto CH, Mecham RP. Functional rescue of elastin insufficiency in mice by the human elastin gene: implications for mouse models of human disease. *Circ Res.* 2007;101:523–531.

# Circulation Research

JOURNAL OF THE AMERICAN HEART ASSOCIATION



## Reduced Vessel Elasticity Alters Cardiovascular Structure and Function in Newborn Mice

Jessica E. Wagenseil, Chris H. Ciliberto, Russell H. Knutsen, Marilyn A. Levy, Attila Kovacs  
and Robert P. Mecham

*Circ Res.* 2009;104:1217-1224; originally published online April 16, 2009;

doi: 10.1161/CIRCRESAHA.108.192054

*Circulation Research* is published by the American Heart Association, 7272 Greenville Avenue, Dallas, TX 75231

Copyright © 2009 American Heart Association, Inc. All rights reserved.

Print ISSN: 0009-7330. Online ISSN: 1524-4571

The online version of this article, along with updated information and services, is located on the  
World Wide Web at:

<http://circres.ahajournals.org/content/104/10/1217>

Data Supplement (unedited) at:

<http://circres.ahajournals.org/content/suppl/2009/04/17/CIRCRESAHA.108.192054.DC1>

**Permissions:** Requests for permissions to reproduce figures, tables, or portions of articles originally published in *Circulation Research* can be obtained via RightsLink, a service of the Copyright Clearance Center, not the Editorial Office. Once the online version of the published article for which permission is being requested is located, click Request Permissions in the middle column of the Web page under Services. Further information about this process is available in the [Permissions and Rights Question and Answer](#) document.

**Reprints:** Information about reprints can be found online at:  
<http://www.lww.com/reprints>

**Subscriptions:** Information about subscribing to *Circulation Research* is online at:  
<http://circres.ahajournals.org/subscriptions/>

## Expanded Materials and Methods

### *Mice*

Newborn pups from crosses of C57BL/6J mice bearing a heterozygous deletion of exon 1 in the elastin gene (*Eln*<sup>+/-</sup>)<sup>1</sup> were used for all studies. Pups were studied and sacrificed 3-24 hours after birth, which allows time for closure of the ductus arteriosus<sup>2</sup>, but is still within the first day of life. This time period is referred to as postnatal day (P)

1. All housing, surgical procedures and experimental protocols were approved by the Institutional Animal Care and Use Committee.

### *Blood Pressure*

P1 pups were anesthetized with 1.5% isoflurane and kept warm by radiant heat. Left ventricular (LV) pressure was measured with a 30G needle connected to a flow through pressure transducer (Uniflow, Baxter). The needle was inserted through the chest wall and into the LV chamber under ultrasound guidance (Vevo 770, Visualsonics, 55 MHz probe). While a parasternal long-axis image of the LV was monitored continuously, the needle was advanced through apical puncture using the injection arm of the Visualsonics imaging platform. This technique allows accurate placement of the needle in the mid LV chamber while avoiding complications of blind percutaneous puncture, such as pneumothorax or pericardial tamponade. After the pressure data were obtained, the needle was retracted under the same ultrasound guidance, and cardiac function was monitored for another minute to ensure hemodynamic stability. The fluid-filled pressure system does not have the dynamic response necessary to acquire the complete waveform at the high heart rates of P1 mice, but a damped pressure waveform was acquired and the

mean LV pressure and heart rate were measured over five cardiac cycles. Assuming that the true LV diastolic pressure is zero, the measured mean pressure is equal to half the systolic pressure.

### *Echocardiography*

For initial echocardiography studies, the anesthetic system was not optimized for the small size of P1 pups and the pups cannot move much, so they were awake during imaging. For later studies, the anesthetic system was adapted for the small pups and it was found that better images could be obtained if the pups were completely immobilized, so they were anesthetized with 1.5% isoflurane. Data was combined for all studies and the anesthetic effects were included in the statistical analysis. All pups were kept warm by radiant heat. Two-dimensional, m-mode and Doppler ultrasound images were obtained with a Vevo 770 ultrasound system and a 55 MHz probe (Visualsonics). Functional parameters were calculated using Visualsonics software and standard equations<sup>3,4</sup>.

### *Morphology and Ultrastructural Analysis*

After sacrifice, the body weight was measured and tail clips were taken for genotyping. The ascending aorta and major branches were imaged with a stereomicroscope coupled to a video camera. For some mice, eosin dye was injected through the LV into the arterial lumen to increase contrast between the arteries and surrounding tissue. The heart was removed and weighed and the aorta was removed for further studies.

For ultrastructural analysis, proximal ascending aortae were fixed in 2.5% glutaraldehyde/0.1 M sodium cacodylate, sequentially stained with osmium tetroxide, tannic acid and uranyl acetate, then dehydrated and embedded in PolyBed 812 (Polysciences). Thin sections (60 nm) were counterstained with uranyl acetate and lead citrate, examined on a Zeiss 902 electron microscope and imaged with Kodak EM film. Two aortae were imaged for each genotype and several grids were examined for each aorta.

#### *DNA amount*

Aortae were cut between the heart and innominate artery and frozen at -80° C until use. DNA was isolated using standard proteinase K methods and quantified using PicoGreen (Invitrogen) and a fluorescent plate reader.

#### *Mechanical Testing*

Mechanical testing was performed using a pressure and force arteriograph (Danish Myotechnology) as described previously for adult arteries<sup>5</sup>. The ascending aorta was mounted at its unloaded length and preconditioned for three cycles. After preconditioning, the intravascular pressure was increased from 0-60 mmHg in steps of 5 mmHg (5 sec/step) for three cycles. For the first protocol, the force either remained constant or decreased with increased pressure, implying that the aorta was either at or below its in vivo length<sup>6</sup>. If the force decreased, the aorta was stretched 2% and the protocol was repeated so that data could be obtained near the in vivo length. After testing, the aorta was removed and 2-3 rings, 0.2-0.3 mm thick were cut to determine the

unloaded dimensions and circumferential residual strain. The rings were placed in physiologic saline solution and unloaded dimensions and circumferential residual strain, as characterized by the opening angle (OA), were measured as described previously<sup>5</sup>.

### *Mechanical Data Analysis*

The *in vivo* length protocol, where the longitudinal force remained approximately constant with increasing pressure<sup>7</sup>, was used for all analyses and comparisons between genotypes. It was difficult to ensure that the aorta returned to a completely unpressurized state between cycles, therefore only data from 5-60 mmHg was included. Compliance for each pressure value was calculated as the average diameter change between that point and the pressure values above and below that point. At the lowest and highest points (5 and 60 mmHg, respectively) only the diameter change above or below that point was used, as necessary. Pressure, longitudinal force and outer diameter from the *in vivo* length protocol were converted to stress and stretch ratios as described previously<sup>5</sup>. Aortae from all genotypes showed constant force with increasing pressure when stretched an average of 1% from their unloaded lengths, hence 1.01 was used as the stretch ratio when calculating the deformed the inner diameter.

### *Statistics*

Outliers that were greater than three standard deviations from the mean were not included in the genotype comparisons. One WT and one *Eln*<sup>+/-</sup> mouse for the pressure data and one WT and two *Eln*<sup>+/-</sup> mice for the compliance data were excluded as outliers. Welch's ANOVA followed by the Tukey-Kramer test were used to determine statistical

differences between genotypes. For the echocardiography data, mixed models followed by the Tukey-Kramer test were used to control for anesthetic effects. SAS/STAT software (SAS Institute Inc.) was used for all analyses and  $P < 0.05$  was considered significant.

## References

1. Li DY, Faury G, Taylor DG, Davis EC, Boyle WA, Mecham RP, Stenzel P, Boak B, Keating MT. Novel arterial pathology in mice and humans hemizygous for elastin. *J Clin Invest.* 1998;102:1783-1787.
2. Tada T, Kishimoto H. Ultrastructural and histological studies on closure of the mouse ductus arteriosus. *Acta Anat (Basel).* 1990;139:326-334.
3. Pombo JF, Troy BL, Russell RO, Jr. Left ventricular volumes and ejection fraction by echocardiography. *Circulation.* 1971;43:480-490.
4. Troy BL, Pombo J, Rackley CE. Measurement of left ventricular wall thickness and mass by echocardiography. *Circulation.* 1972;45:602-611.
5. Wagenseil JE, Nerurkar NL, Knutsen RH, Okamoto RJ, Li DY, Mecham RP. Effects of elastin haploinsufficiency on the mechanical behavior of mouse arteries. *Am J Physiol Heart Circ Physiol.* 2005;289:H1209-17.
6. Humphrey JD. *Cardiovascular Solid Mechanics.* New York: Springer-Verlag; 2002.
7. Dye WW, Gleason RL, Wilson E, Humphrey JD. Altered biomechanical properties of carotid arteries in two mouse models of muscular dystrophy. *J Appl Physiol.* 2007;103:664-672.

**Legend for Online Movie.**

*Eln*<sup>-/-</sup> mice have a long tortuous aorta. Ultrasound images of the ascending (AA) and descending (DA) aorta are shown for each genotype. Note the hairpin turn in the *Eln*<sup>-/-</sup> aorta at the transition between the ascending and descending regions (\*). The scale on the right is in mm.